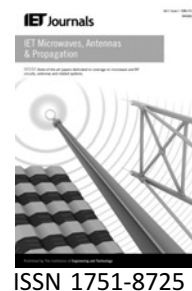


Published in IET Microwaves, Antennas & Propagation
 Received on 13th August 2007
 Revised on 6th April 2008
 doi: 10.1049/iet-map:20080052



Analytical modelling of microstrip-like interconnections in presence of ground plane aperture

R. Sharma¹ T. Chakravarty² A.B. Bhattacharyya³

¹Jaypee University of Information Technology, Wazirpur, UP 201307, India

²Tata Consultancy Services, Bangalore, KA 560067, India

³Jaypee Institute of Information Technology University, Noida, UP 201307, India

E-mail: tap_chak@vsnl.net

Abstract: High-speed multichip module interconnects are characterised by planar transmission lines. An interconnect line with ground plane aperture is essentially a microstrip line with partially removed ground plane below the line. The authors report the closed-form analytical expressions for line capacitance and characteristic impedance of microstrip interconnect line with a ground plane aperture. The expressions have been obtained using variational analysis combined with transverse transmission line technique. The closed-form expressions are general and are obtained for a range of structure parameters and the dielectric constants. Results are compared with finite-difference time-domain simulations and measurements performed on a vector network analyser. The proposed study can find applications in the design of high-speed interconnects for printed circuit boards, radio frequency (RF) and multichip module applications. These are particularly useful where high impedance lines are required.

1 Introduction

Planar transmission lines form the basic media for multichip module interconnections. A microstrip line is an inhomogeneous transmission line structure. It consists of a strip conductor on a flat dielectric substrate with a metallic ground plane on its reverse side. The characteristic impedance Z of the microstrip line is given by $Z = Z_a / \sqrt{\epsilon_{\text{eff}}}$, where Z_a is the characteristic impedance of the microstrip line with the dielectric replaced by air [1–5]. Here, ϵ_{eff} is the effective dielectric constant of the medium, and its value lies in the range $1 < \epsilon_{\text{eff}} < \epsilon_r$, where ϵ_r is the dielectric constant of the substrate. At low frequency, the mode of propagation resembles the TEM mode, and hence, is termed as the quasi-TEM mode. Because of this quasi-TEM mode approximation, the calculation of propagation parameters of the line reduces to the solution of the two-dimensional Laplace's equation. Several analytical methods are reported in the available literature [6–30]. Most important among them are the conformal transformation method [6], the variational method [6–8],

the finite-difference method [9, 10], the finite-element method [11] and the finite-difference time-domain (FDTD) techniques [25–30]. These analytical methods have traditionally been used for the analysis of general microstrips, high-speed digital lines and microstrip-like interconnects.

Traditionally, it is found that the characteristic impedance of a microstrip line is related to width of the strip, height of the substrate and the dielectric constant of the substrate. Although various analytical techniques are available for planar transmission line interconnects, the effect of ground plane aperture on the computation of characteristic impedance has not been reported till now. Ground plane aperture is normally referred to partial removal of the ground plane below the interconnect line. Introduction of such an aperture in the ground plane below the strip, changes the line properties significantly; in that the characteristic impedance of the line increases with increase in the aperture size. A typical lateral view of such an interconnect structure is shown in Fig. 1. Introduction of

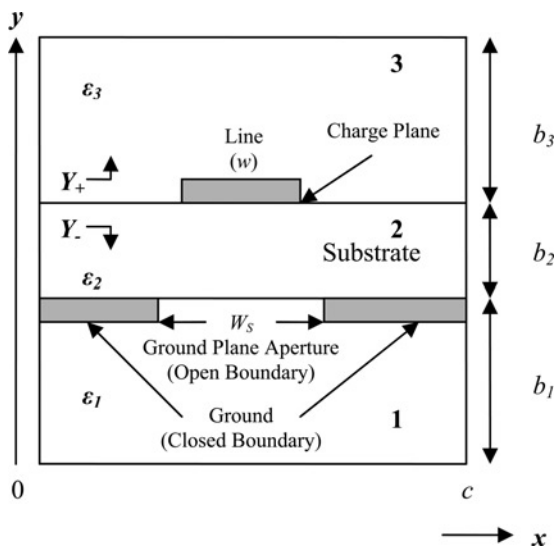


Figure 1 Lateral view of the interconnect structure

a ground plane aperture can thus provide additional flexibility to printed circuit board (PCB) designers in ensuring desired line impedance and therefore optimum signal integrity. We use the variational method in space domain combined with the transverse transmission line technique (unified method) in our analysis as it offers the most general and the simplest approach to such class of problems. The expressions are general and can be used for a class of such structures irrespective of the number of dielectric layers [1]. Use of ground plane aperture has interesting applications such as 3 dB edge coupler [31], band-pass filters [32, 33] and microstrip line-based split ring [34–37], where this analysis can be useful for designers.

In this paper, we report the closed-form expressions for microstrip-like interconnects taking into consideration the effects of ground plane aperture. The line capacitance is computed using variational method combined with transverse transmission line technique [1, 8]. Results are validated by FDTD simulations and measurements performed on a vector network analyser. As a special case, the results show good agreement with the design data in the available literature for microstrip line [38].

The organisation of the paper is as follows: In Section 2, we present the method of analysis of the interconnect line with ground plane aperture. Section 3 provides analytical results, which are compared with FDTD simulations and measured data. Section 4 provides an insight into the proposed methodology – in that upper bounds for the proposed solution are presented. The paper concludes in Section 5.

2 Method of analysis

Consider the interconnect structure shown in Fig. 1, with an electric wall separation ‘ c ’ forming an enclosed cavity with part opening due to an aperture in the ground plane. Fig. 1

shows a three layer vertical structure represented by dielectric layers 1 (ϵ_1, b_1), 2 (ϵ_2, b_2) and 3 (ϵ_3, b_3), respectively, where ϵ is the permittivity and b is the thickness of the dielectric layers. The geometry of the proposed structure that is an interconnect line with symmetrical ground plane aperture is represented by an interconnect line at the interface between regions 2 and 3 and the partial ground plane projection at the interface between regions 1 and 2. For a microstrip structure, region 1 has no role since the interface between regions 1 and 2 contains a ground plane from end to end wall. On the other hand, for suspended stripline structure, all the three regions enclosed by the shielding walls play a role in the computation of parameters like characteristic impedance. In this paper, the structure proposed is a microstrip line with ground plane aperture. Therefore this problem is approached by considering both the cases of microstrip and suspended stripline structures. From Fig. 1, one is able to see that the proposed structure is non-homogeneous. This is due to the fact that the ground extends to a certain distance below the substrate from the end walls with partial opening, indicated as ground plane aperture symmetrically located below the transmission line on the charge plane. Based on this reasoning, we divide the region 2 into three vertical profiles as shown in Fig. 2 namely I, II and III, respectively. Individual admittances of the three vertical profiles computed on the charge plane that is the interface between regions 2 and 3 are parallel to each other. For computation of characteristic impedance of the line, first, we consider the regions 2 and 3 with finite thickness (b_2 and b_3) and permittivity (ϵ_2 and ϵ_3), as shown. The admittance measured on the charge plane (interconnect line) due to these two regions are denoted as Y_- and Y_+ , respectively. While region 3 is homogenous, region 2 is not. Thus the admittance represented by Y_- is a parallel combination of admittances on the charge plane because of the three vertical profiles. It should be noted that Bhat and Koul [1, 38] have considered electric walls on both sides for a given structure with boundary condition $G = 0$, where G is the Green's function [39]. However, there are three possible boundary conditions that should be considered in our analysis.

- Case (a): Electric walls at $x = 0$ and c

$$\beta_n = \frac{n\pi}{c}$$

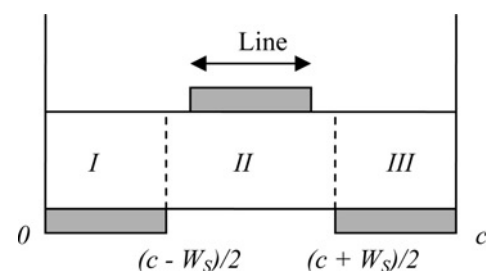


Figure 2 Vertical profiles in region 2

- *Case (b)*: Magnetic walls at $x = (c - W_s)/2$ and $(c + W_s)/2$

$$\beta_n = \frac{n\pi}{W_s}$$

- *Case (c)*: Electric wall at $x = 0$ and magnetic wall at $x = (c - W_s)/2$

$$\beta_n = \frac{(2n + 1)\pi}{2g}$$

where $n = 1, 3, 5, \dots, \infty$ and $g = (c - W_s)/2$.

The detailed formulation for the computation of capacitance using unified approach (variational technique and transverse transmission line technique) is given in the appendix. Hence, only salient steps leading to the computation of the admittance of the interconnect structure are given below. Region 3 is a homogeneous medium with electric walls at $x = 0$ and c and $\epsilon_3 = 1$ (air). The admittance of this region is given by

$$Y_+ = \epsilon_0 \epsilon_3 \coth(\beta_n b_3) \quad (1)$$

where β_n is defined by case (a) as above.

To obtain a microstrip-like structure, we have considered an open structure at the top ($b_3 \gg b_2$). The admittance of region 2 is given by

$$Y_- = Y_I + Y_{II} + Y_{III} \quad (2)$$

where

$$Y_{II} = \epsilon_0 \epsilon_2 \tanh(\alpha_n b_2) \quad (3)$$

$$Y_I = Y_{III} = \epsilon_0 \epsilon_2 \coth(\gamma_m b_2) \quad (4)$$

where

$$\alpha_n = \frac{n\pi}{W_s} \quad \text{and} \quad \gamma_m = \frac{m\pi}{g}, \quad \text{where } n = 1, 3, \dots,$$

$$m = 2, 4, \dots \quad \text{and} \quad g = (c - W_s)/2$$

The total admittance of the interconnect structure with the ground plane aperture is given by

$$Y = Y_+ + Y_- \quad (5)$$

Unlike earlier reported works, this expression takes into account the width of the ground plane aperture (W_s). Readers should note that throughout our analysis the aperture length is the same as the line length. The trial function $f(x)$, given in [1, 38], is quite accurate and appropriate for our analysis. The generalised expressions for

the line capacitance C is given by

$$C = \frac{(1 + 0.25A)^2}{\sum_{\text{nodd}} \left((L_n + AM_n)^2 P_n / Y \right)} \quad (6)$$

where

$$L_n = \sin\left(\frac{\beta_n \tau w}{2}\right)$$

$$M_n = \left(\frac{2}{\beta_n \tau w}\right)^3 \left[3 \left\{ (\beta_n \tau w / 2)^2 - 2 \right\} \cos(\beta_n \tau w / 2) + (\beta_n \tau w / 2) \left\{ (\beta_n \tau w / 2)^2 - 6 \right\} \sin(\beta_n \tau w / 2) + 6 \right]$$

$$P_n = \left(\frac{2}{n\pi}\right) \left(\frac{2}{\beta_n \tau w}\right)^2$$

$$\beta_n = \frac{n\pi}{c}$$

$$A = -\frac{\sum_{\text{nodd}} (L_n - 4M_n) L_n P_n / Y}{\sum_{\text{nodd}} (L_n - 4M_n) M_n P_n / Y}$$

(7)

and

$$n = 1, 3, \dots, 10001$$

Detailed derivation of (6) is given in the appendix. The above expression takes into account the ground plane aperture (GPA) width W_s . It may be of interest to the reader that the variation in the size of the aperture leads to reduction in the line to ground capacitance. This results in the overall increase in the values of Z with respect to the aperture width W_s . As the GPA width W_s reduces to zero, the solution corroborates to standard microstrip line analysis. This happens to be a special case in our analysis, results of which are compared with standard microstrip design data [38] in the following section. The analysis presented above is valid for homogeneous, isotropic and lossless medium. Note that the capacitance formula in our case changes from that in the earlier reported literature as it incorporates the ground plane aperture width (W_s). The characteristic impedance Z can now be computed as $Z = 1/v^a \sqrt{CC_a}$ [8]. Here, C is the capacitance per unit length of the structure, C_a is the capacitance per unit length of the structure with all dielectrics replaced by air, and v^a is the velocity of propagation in air. In the following section, we discuss the results obtained from the above formulation.

3 Results

Using (1–7), we can obtain the characteristic impedance of the proposed structure. In the following subsection, the analytical results obtained above are compared with FDTD simulations and measurements.

(a) *Comparative plots:* Fig. 3 shows a comparative plot of the characteristic impedance for different dielectric materials. The comparative results shown in Fig. 3 are obtained for different substrates with the dielectric constant (ϵ_r) ranging from 2.2 to 11.9. The results are obtained with an electric wall separation far more than the ground plane aperture width. Introduction of an aperture in the ground plane below the line leads to reduction in the line to ground capacitance, thereby increasing the characteristic impedance of the line. The results obtained in this section are valid for a range of dielectric materials ($2.2 \leq \epsilon_r \leq 12$) and $b_2/\lambda_g \leq 0.02$, where λ_g is the guide wavelength. The comparison with FDTD simulation results in Fig. 3 proves the accuracy of our analysis. The results are also validated by comparing our proposed theoretical results with measured data. The results are fairly accurate for both $w/b_2 \leq 1$ and $w/b_2 \geq 1$, for dielectric constants upto 12 and GPA width $W_s \leq 10$ mm.

(b) *Experimental results:* Fabrication of the interconnect structure is done on a standard FR4 substrate ($\epsilon_r = 4.6$, line length = 14 mm, line width 'w' = 4 mm, and $b_2 = 1.59$ mm). The measurements were performed on a vector network analyser. Considering a load resistance of 50 Ω , the characteristics impedance of the line is calculated from the input impedance and is provided in Table 1. Table 1 shows a comparison between the analytical results obtained using variational analysis, FDTD simulation data and the measured data for the fabricated structure with three different aperture widths.

It is seen that the computed values of characteristic impedance from the formulation used in this work is

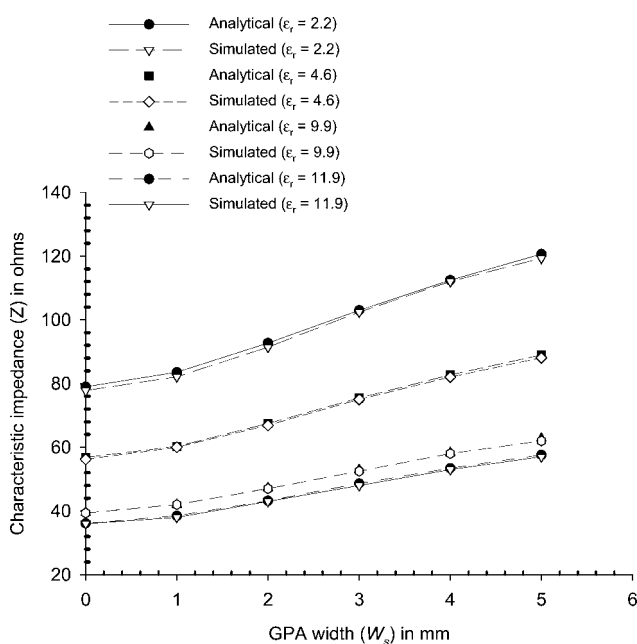


Figure 3 Characteristic impedance of the line as a function of aperture width (length = 1 mm, $w = 0.76$ mm and $b_2 = 0.508$ mm)

Table 1 Characteristic impedance Z obtained by measurement, simulation and proposed formulation

W_s , mm	Measured results, Ω	FDTD simulation results, Ω	Theoretical results, Ω
3	44.14	44.23	44.69
4	46.91	45.97	46.39
5	48.51	48.06	48.42

within $\pm 2\%$ accuracy. When the width of the GPA (W_s) is reduced to zero, the same formulation can be used for the analysis of microstrip lines. As a special case, we now compare our results with those obtained using Wheeler's formula for a standard microstrip line [2–4].

Let $\epsilon_3 = 1$, $\epsilon_2 = \epsilon_r$ and $b_3 \gg b_2$. Table 2 shows a comparison between the proposed results and those obtained using Wheeler's formula for a microstrip line.

4 Analysis of the proposed methodology

One of the assumptions made in our analysis is the placement of magnetic walls. Although the numerical computation based on this assumption provides accurate results, it is worth investigating the accuracy of this hypothesis. For such evaluation, field simulator is used to plot the H-field when a line with GPA is excited. It is clearly seen from the results that the tangential component of H-field goes to zero on such boundaries thus validating our assumptions. In Fig. 4, the contour plot of the z-directed H-field is shown on the cross-section plane mid-way through the length of the terminated line (in this case, the length of the line is 1 mm). This component of H-field is represented in terms of isoline. Closely reading the amplitudes of the H-field, it is seen that the assumption of magnetic wall is approximately valid if we consider the relative ratio of amplitudes of peak and the edge values. Of course, a perfect magnetic wall (PMC) boundary condition cannot be met but it is a reasonable mathematical assumption which simplifies the computation of the characteristic impedance.

Table 2 Comparison of characteristic impedance Z for a microstrip line ($b_3/b_2 \gg 1$, $\epsilon_r > = 3.78$)

w/b_2	Proposed results, Ω	Wheeler's formula [2–4], Ω
0.8	83.18	83.74
1.3	66.91	66.23
1.4	62.23	63.7
1.5	59.43	61.37
1.6	58.62	59.21

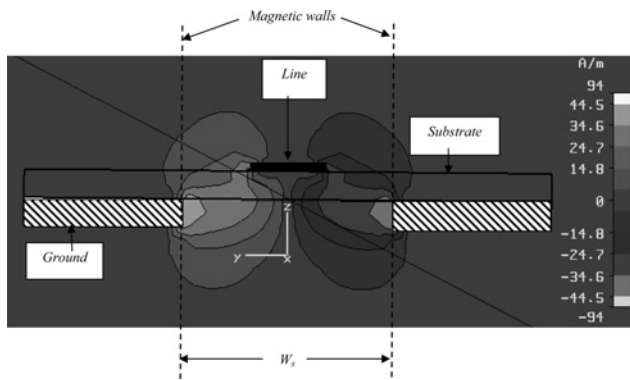


Figure 4 Amplitude of z -directed (tangential) component of H -field on the cross-section plane ($w = 1.5$ mm, length = 1 mm, $W_s = 4$ mm, $\epsilon_r = 2.2$, $b_2 = 0.508$ mm and $f_{sim} = 1$ GHz)

Partially removing the ground plane will induce higher-order modes. Therefore the utility of the proposed structure as a planar transmission line, considering only the quasi-static TEM mode, needs to be studied extensively. In a microstrip line, for dominant modes to exist without including any higher-order modes, the substrate thickness must be less than a critical value. Apart from higher-order modes of propagation, microstrip line also exhibits variation in characteristic impedance with respect to the frequency; mainly because of dispersion effects. Thus, it becomes all the more necessary to predict an upper bound for the practical use of this methodology. This study is carried out using FDTD simulations and the results are presented below. Taking hint from FDTD simulation, we establish upper bounds; namely the range of frequency, over which our method will hold well.

The line width (w) is 0.76 mm and the ground plane aperture width (W_s) is 1 mm with $\epsilon_r = 9.9$, 4.6 and 2.2. For each substrate type, three different substrate thicknesses are considered ($b_2 = 0.508$, 1.59 and 3.2 mm). Figs. 5–7 show the variation in characteristic impedance with respect to frequency. In these plots, the straight lines correspond to the calculated characteristic impedance computed using our formulation, which happens to be independent of frequency. However, in all such cases, full-wave simulation displays a monotonic variation in characteristic impedance owing to frequency dispersion effects. This is attributed to the difference observed between the simulated and analytical results depicted in Figs. 5–7. Our proposed analysis can give fairly accurate results up to a few GHz in the worst case. The results clearly bring forth the fact that the use of lower dielectric constant materials with thinner substrates extends the frequency range of operation of this structure with the exclusion of higher-order modes. Generally, GPA limits the upper frequency use of interconnect structures when compared with ordinary microstrip structures. For an alumina substrate ($\epsilon_r = 9.9$) and substrate height $b_2 = 3.2$ mm, the analytical results are accurate up to 1.6 GHz. For other materials and substrate heights, the upper bound of useful frequency is even higher. It may be of

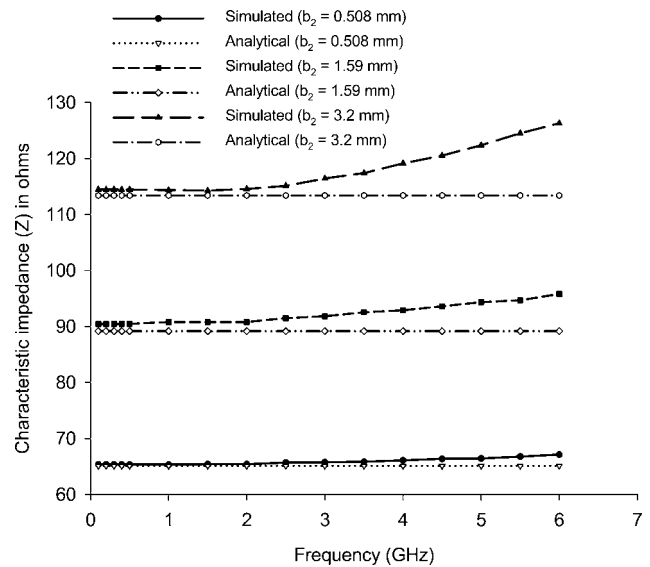


Figure 5 Characteristic impedance against frequency ($\epsilon_r = 2.2$, length = 4 mm, $w = 0.76$ mm and $W_s = 1$ mm)

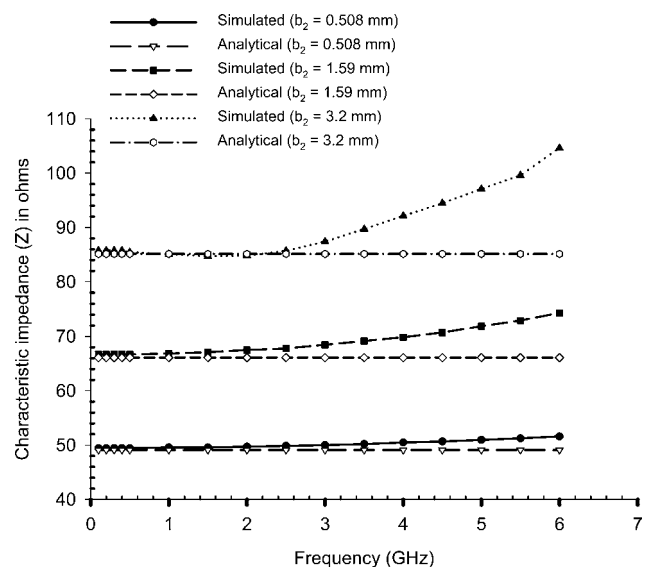


Figure 6 Characteristic impedance against frequency ($\epsilon_r = 4.6$, length = 4 mm, $w = 0.76$ mm and $W_s = 1$ mm)

interest to the reader that modern day interconnects are commonly used to carry signals of frequencies of the order of a few GHz only. In Figs. 5–7, we try to bring forth the upper bound of frequency for various interconnect geometries for which our analysis can be used without taking frequency dispersion into consideration.

The effects of frequency dispersion will also vary with the ground plane aperture width (W_s) and are given in Fig. 8. Microstrip line with ground plane aperture of varying width is compared with a simple conventional microstrip line. It is seen that larger the aperture, lower is the frequency range of operation.

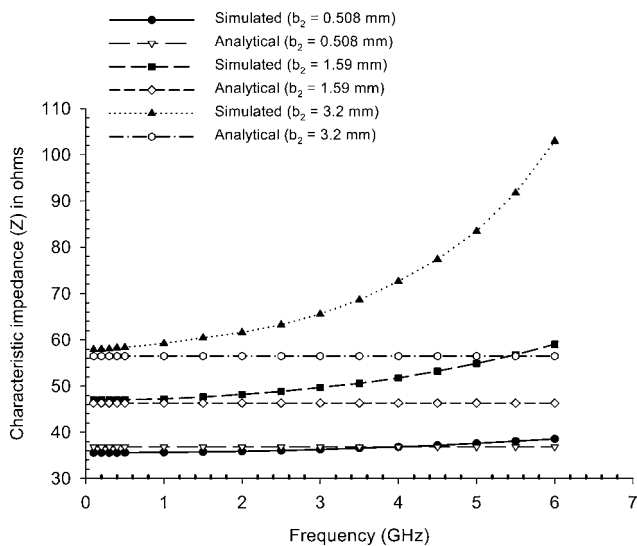


Figure 7 Characteristic impedance against frequency ($\epsilon_r = 9.9$, length = 4 mm, $w = 0.76$ mm and $W_s = 1$ mm)

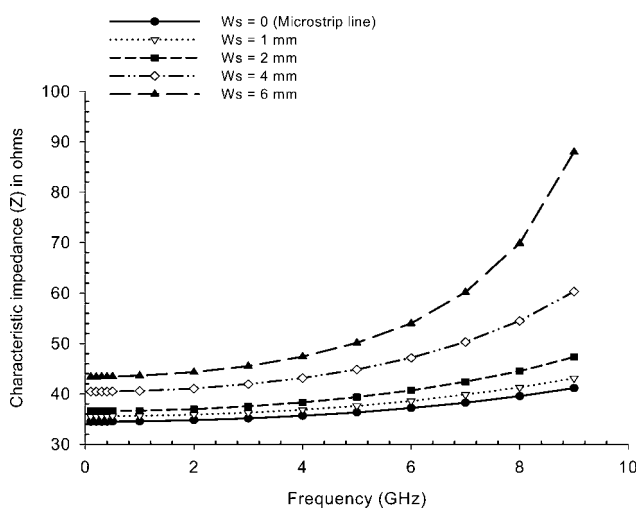


Figure 8 Characteristic impedance against frequency for different aperture widths ($\epsilon_r = 9.9$, length = 1 mm, $w = 0.76$ mm and $b_2 = 0.508$ mm)

The proposed analytical model for computing characteristic impedance has a lot of significance which are outlined below.

- The proposed model can serve as a first hand synthesis procedure for a designer, which can be followed by full-wave accurate simulation to check the veracity of the design. Our present approach, once programmed will generate results much quickly and fairly accurately.
- The analytical approach can also be used to extract the distributed capacitance and inductance of the interconnect line, thereby facilitating transient response for step and impulse inputs. Similarly, the method can be extended to extract the coupling capacitances and predict the cross-talk without much significant computational effort.

- Transmission line with GPA has potential applications in filters and couplers where tighter coupling values can be obtained using this approach. For all such applications, the computation of characteristic impedance for a single line can be the beginning point of the design.

In the worst case, the full-wave simulations show that our proposed method, which does not take into account the frequency dispersion, shows reasonably accuracy up to 3 GHz for all types of structures. This generally happens to be the working range of frequencies in printed circuit board (PCB) and radio frequency integrated circuit (RFIC) interconnects. We can summarise the above discussion by stating that the unified approach to computation of characteristic impedance for microstrip-like interconnects with ground plane aperture is valid for the following cases

- $2.2 \leq \epsilon_r \leq 12$.
- $b_2/\lambda_g \leq 0.02$.

5 Conclusion

In this paper, a microstrip-like interconnects line in presence of a ground plane aperture is analysed using unified method. The characteristic impedance of the line changes significantly with varying size of the ground plane aperture. The theoretical results are compared with experimental data and FDTD simulations, which demonstrate the accuracy of the proposed formulation. As a special case, the results converge to available microstrip line model. Analysis is presented to consider the effects of higher-order modes using FDTD simulation. However, it should be cautioned that the introduction of GPA might limit the upper frequency range of the interconnect line. However, for thinner substrates with lower dielectric constants, this upper bound is reasonably good.

The proposed analytical approach to solve this problem has its own uses and since the presented problem has not been solved by others using any other analytical approach (to the best of our knowledge); the method itself deserves a consideration. The proposed expressions do not use any special function. The proposed formulation will be useful in design and analysis of high-speed multichip module interconnects, as well as multilayer PCB and RFICs with, optimum signal integrity. Applications can also be found in millimetre wave components which require shorter electrical lengths, and microwave components such as directional couplers, band-pass filters and split rings.

6 References

- [1] BHAT B., KOUL S.K.: 'Unified approach to solve a class of strip and microstrip-like transmission lines', *IEEE Trans. Microw. Theory Tech.*, 1982, **82**, (5), pp. 679–686

- [2] WHEELER H.A.: 'Transmission-line properties of parallel strips separated by a dielectric sheet', *IEEE Trans. Microw. Theory Tech.*, 1965, **13**, (2), pp. 172–185
- [3] WHEELER H.A.: 'Transmission-line properties of parallel wide strips by a conformal mapping approximation', *IEEE Trans. Microw. Theory Tech.*, 1964, **12**, (3), pp. 280–289
- [4] WHEELER H.A.: 'Transmission-line properties of a strip on a dielectric sheet on a plane', *IEEE Trans. Microw. Theory Tech.*, 1977, **25**, (8), pp. 631–647
- [5] EDWARDS T.C.: 'Foundations of microstrip circuit design' (Wiley, New York, 1981)
- [6] PIPES L.A.: 'Applied mathematics for engineers and physicists' (McGraw-Hill, New York, 1958)
- [7] YAMASHITA E., MITTRA R.: 'Variational method for the analysis of microstrip lines', *IEEE Trans. Microw. Theory Tech.*, 1968, **16**, (4), pp. 251–256
- [8] COLLIN R.E.: 'Field theory of guided waves' (McGraw-Hill, New York, 1960)
- [9] GREEN H.E.: 'The numerical solution of some important transmission line problems', *IEEE Trans. Microw. Theory Tech.*, 1965, **13**, (5), pp. 676–692
- [10] SCHNEIDER M.V.: 'Computation of impedance and attenuation of TEM-lines by finite-difference methods', *IEEE Trans. Microw. Theory Tech.*, 1965, **13**, (6), pp. 793–800
- [11] SHIH C., WU R.-B., JENG S.-K., CHEN C.H.: 'A full-wave analysis of microstrip lines by variational conformal mapping technique', *IEEE Trans. Microw. Theory Tech.*, 1988, **36**, (3), pp. 576–581
- [12] CHANG C.-N., CHENG J.-F.: 'Full-wave analysis of multilayer microstrip lines', *IEE Proc. Microw. Antennas Propag.*, 1994, **141**, (3), pp. 185–188 June
- [13] LIN S.-Y., LEE C.C.: 'A full wave analysis of microstrips by the boundary element method', *IEEE Trans. Microw. Theory Tech.*, 1996, **44**, (11), pp. 1977–1983
- [14] MITKEES A.A., HINDY M.A.: 'Characteristic impedance for finite length microstrip line'. Proc. 32nd Midwest Symp. Circuits and Systems, August 1989, pp. 1050–1052
- [15] CHANG C.-N., CHENG J.-F.: 'Hybrid quasistatic analysis of multilayer microstrip lines', *IEE Proc., H Microw. Antennas Propag.*, 1993, **140**, (2), pp. 79–83
- [16] KIANG J.-F.: 'Quasistatic analysis of microstrip lines on lossy inhomogeneous substrates', *IEE Proc., Microw. Antennas Propag.*, 1996, **143**, (5), pp. 379–384
- [17] FENG N.N., FANG D.G., HUANG W.P.: 'An approximate analysis of microstrip lines with finite metallization thickness and conductivity by method of lines'. Microwave and Millimetre Wave Technology Proc., August 1998, pp. 1053–1056
- [18] DREHER A., IOFFE A.: 'Analysis of microstrip lines in multilayer structures of arbitrary varying thickness', *Microw. Guided Wave Lett.*, 2000, **10**, (2), pp. 52–54
- [19] TRAN A.M., ITOH T.: 'Analysis of microstrip lines coupled through an arbitrary shaped aperture in a thick common ground plane', *IEEE MTT-S Int. Microw. Symp. Digest*, 1993, pp. 819–822
- [20] TRAN A.M., HOUSHMAND B., ITOH T.: 'Analysis of microstrip lines coupled through an arbitrary circular aperture in a thick common ground plane'. Electrical Performance of Electronic Packaging Proc., October 1993, pp. 19–21
- [21] MA Z., YAMASHITA E., XU S.: 'Hybrid-mode analysis of planar transmission lines with arbitrary metallization cross sections', *IEEE Trans. Microw. Theory Tech.*, 1993, **41**, (3), pp. 491–497
- [22] KIM J.-S., PARK W.S.: 'Efficient analysis of microstrip lines including edge singularities in spatial domains', *IEEE Microw. Wirel. Compon. Lett.*, 2001, **11**, (6), pp. 270–272
- [23] KAPOOR S.: 'Sub-cellular technique for finite-difference time-domain method', *IEEE Trans. Microw. Theory Tech.*, 1997, **45**, (5), pp. 673–677
- [24] CHEN Z.-H., CHU Q.-X.: 'A novel FDTD matched load model of microstrip line'. Asia Pacific Microwave Conf. Proc., December 2005, vol. 3
- [25] ARIMA T., UNO T.: 'Modification of FDTD method for highly accurate analysis of microstrip lines using quasi-static approximation'. IEEE Antennas and Propagation Society Int. Symp., 2006, pp. 2771–2774
- [26] XIAODONG H., ANPING Z., DALI L., SHAOHUA H., DONGJIANG W., RONGJIN Y.: 'Analysis of microstrip line and optical waveguide with the two-dimensional finite difference time domain method'. Int. Conf. Communication Technology Proc., August 2000, vol. 2, pp. 1565–1570
- [27] SCARLATTI A., HOLLOWAY C.L.: 'An equivalent transmission-line model containing dispersion for high-speed digital lines – with an FDTD implementation', *IEEE Trans. Electromagn. Compat.*, 2001, **43**, (4), pp. 504–514
- [28] YOON J.-G., DIB N.I., RATEHI L.P.B.: 'Characterization of high frequency interconnects using finite difference time domain and finite elements methods', *IEEE Trans. Microw. Theory Tech.*, 1994, **42**, (9), pp. 1727–1736

- [29] YOU S.-H., KUESTER E.F.: 'Fast and direct coupled-microstrip interconnect reduced-order modeling based on the finite-element method', *IEEE Trans. Microw. Theory Tech.*, 2006, **54**, (5), pp. 2232–2242
- [30] LAM C.-W., ALI S.M., NUYTKENS P.: 'Three-dimensional modeling of multichip module interconnects', *IEEE Trans. Compon. Hybrids Manuf. Technol.*, 1993, **16**, (7), pp. 699–704
- [31] SHARMA R., CHAKRAVARTY T., BHOOSHAN S., BHATTACHARYYA A.B.: 'Design of a novel 3 db microstrip backward wave coupler using defected ground structure', *Prog. Electromagn. Res.*, 2006, **65**, pp. 261–273,
- [32] MANDAL M.K., SANYAL S.: 'Design of wide-band, sharp-rejection bandpass filters with parallel-coupled lines', *IEEE Microw. Wirel. Compon. Lett.*, 2006, **16**, (11), pp. 597–599
- [33] MANDAL M.K., MONDAL P., SANYAL S., CHAKRABARTY A.: 'Low insertion-loss, sharp-rejection and compact microstrip low-pass filters', *IEEE Microw. Wirel. Compon. Lett.*, 2006, **16**, (11), pp. 600–602
- [34] YING X., ALPHONES A.: 'Design of microstrip line based split ring PBG structures'. IEEE Int. Workshop on Antenna Technology: Small Antennas and Novel Metamaterials, March 2005, pp. 426–430
- [35] TAM W.Y., CHEN Y.: 'Analysis of microstrip lines on a perforated ground using reciprocity method'. Asia Pacific Microwave Conf. Proc., 1997, vol. 1, pp. 425–428
- [36] LASO A.G., ERRO M.J., SOROLLA M., THUMM M.: 'Analysis and design of periodic structures for microstrip lines by using the coupled mode theory', *IEEE Microw. Wirel. Compon. Lett.*, 2002, **12**, (11), pp. 441–443
- [37] HOFSCHEIN S., WOLFF I.: 'Simulation of an elevated coplanar waveguide using 2-D FDTD', *IEEE Microw. Guided Wave Lett.*, 1996, **6**, (1), pp. 28–30
- [38] BHAT B., KOUL S.K.: 'Stripline-like transmission lines for microwave integrated circuits' (Wiley, New York, 1989)
- [39] CRAMPAGNE R., AHMADPANA M., GUIRAUD J.-L.: 'A simple method for determining the green's function for a large class of MIC lines having multilayered dielectric substrates', *IEEE Trans. Microw. Theory Tech. and Tech.*, 1978, **26**, (2), pp. 82–87

7 Appendix: capacitance extraction formulation of the interconnect structure

Extensive literature is available for the analytical and numerical solutions of microstrip-like transmission line

interconnects. While the hybrid mode approach is rigorous and complicated, the quasi-static approach is simpler although limited to lower frequency applications. For the analysis of interconnects such as the one shown in Fig. 1, the variational analysis method is found to be the simplest [1, 8]. This requires the computation of either the potential function or the Green's function in a given configuration. The complete derivation for various single and coupled-line structures is provided by Bhat and Koul in [1], whereas standard formulas for line impedance Z is given in [8] and a part of these is reproduced here.

Consider the interconnect structure shown in Fig. 9. The Green's function $G(x, y/x_0, y_0)$ due to a unit charge located at (x_0, y_0) satisfies the Poisson's differential equation

$$\nabla^2 G(x, y/x_0, y_0) = (-1/\epsilon)\delta(x - x_0)\delta(y - y_0) \quad (8)$$

where $\delta(x - x_0)$ and $\delta(y - y_0)$ are Dirac's delta functions and ϵ is the dielectric constant of the region containing the charge. The Green's function can be expressed as

$$G(x, y/x_0, y_0) = \sum_n \sin(\beta_n x) G_n(y) \quad (9)$$

Substituting (9) in (8), $G_n(y)$ satisfies the following equation

$$(d^2/dy^2 - \beta_n^2)G_n(y) = -(2/c\epsilon) \sin(\beta_n x_0)\delta(y - y_0) \quad (10)$$

Solving (10) using transverse transmission line method [1], we have

$$G_n(y) = (2/\beta_n c Y) \sin(\beta_n x_0) \quad (11)$$

where Y is the admittance at the charge plane, $y = y_0$. Here, Y is the sum of admittances Y_+ and Y_- . Substituting (11) in (9), the Green's function at the charge plane $y = y_0$, is given as

$$G(x, y/x_0, y_0) = \sum_{n=1}^{\infty} (2/n\pi Y) \sin(\beta_n x) \sin(\beta_n x_0) \quad (12)$$

The capacitance of the interconnect structure shown in Fig. 9

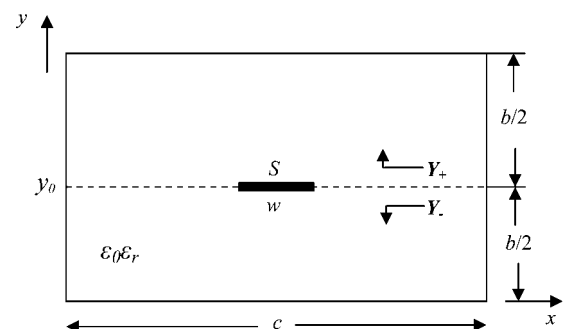


Figure 9 Lateral view of a general microstrip-like interconnect structure

is obtained using (12) in the following variational expression [1, 38]

$$\frac{1}{C} = \frac{\int_S \int_S G(x, y_0/x_0, y_0) f(x) f(x_0) dx dx_0}{[\int_S f(x) dx]^2} \quad (13)$$

where $f(x)$ is the charge distribution on the line (S) and is given as

$$f(x) = \begin{cases} \left(\frac{1}{w}\right) [1 + A|(2/w)(x - c/2)|^3], & \text{for } (c - w)/2 \leq x \\ & \leq (c + w)/2 \\ \text{and} & \\ = 0, & \text{otherwise} \end{cases} \quad (14)$$

where A is an arbitrary constant and is determined by maximising the line capacitance C . Substituting (12) and (14) in (13) and evaluating the integral, we obtain the set of expressions given as (6) and (7) in Section 2 of the text.

The characteristic impedance Z can now be computed as given in [8]. Here, C is the capacitance per unit length of the structure, C_a is the capacitance per unit length of the structure with all dielectrics replaced by air and v^a is the velocity of propagation in air. Because of an aperture introduced in the ground plane, modified boundary conditions require the recalculation of the admittance Y (Y_+ and Y_-) in our case. The modified boundary conditions and the admittance parameters are given in Section 2 of the text.